Preliminary Communication

For reprint orders, please contact: reprints@future-science.com

Future Medicinal Chemistry

Discovery of novel and potent InhA inhibitors by an *in silico* screening and pharmacokinetic prediction

Chayanin Hanwarinroj[1], Nareudon Phusi[1], Bundit Kamsri[1], Pharit Kamsri[2], Auradee Punkvang[2], Sombat Ketrat[3], Patchreenart Saparpakorn[4], Supa Hannongbua[4], Khomson Suttisintong[5], Prasat Kittakoop[6,7,8], James Spencer[9], Adrian J Mulholland[10] & Pornpan Pungpo*[,1]

[1]Department of Chemistry, Faculty of Science, Ubon Ratchathani University, Ubon Ratchathani, 34190, Thailand
[2]Division of Chemistry, Faculty of Science, Nakhon Phanom University, Nakhon Phanom, 48000, Thailand
[3]School of Information Science & Technology, Vidyasirimedhi Institute of Science & Technology, Rayong, 21210, Thailand
[4]Department of Chemistry, Faculty of Science, Kasetsart University, Bangkok, 10900, Thailand
[5]National Nanotechnology Center, NSTDA, Pathum Thani, 12120, Thailand
[6]Chulabhorn Research Institute, Bangkok, 10210, Thailand
[7]Chulabhorn Graduate Institute, Chemical Biology Program, Chulabhorn Royal Academy, Bangkok, 10210, Thailand
[8]Center of Excellence on Environmental Health & Toxicology (EHT), CHE, Ministry of Education, Bangkok, 10300, Thailand
[9]School of Cellular & Molecular Medicine, Biomedical Sciences Building, University of Bristol, Bristol, BS8 1TD, United Kingdom
[10]Centre for Computational Chemistry, School of Chemistry, University of Bristol, Bristol, BS8 1TS, United Kingdom
*Author for correspondence: pornpan_ubu@yahoo.com

Aim: *In silico* screening approaches were performed to discover novel InhA inhibitors. **Methods:** Candidate InhA inhibitors were obtained from the combination of virtual screening and pharmacokinetic prediction. In addition, molecular mechanics Poisson–Boltzmann surface area, molecular mechanics Generalized Born surface area and WaterSwap methods were performed to investigate the binding interactions and binding energy of candidate compounds. **Results:** Four candidate compounds with suitable physicochemical, pharmacokinetic and antibacterial properties are proposed. The crucial interactions of the candidate compounds were H-bond, pi–pi and sigma–pi interactions observed in the InhA binding site. The binding affinity of these compounds was improved by hydrophobic interactions with hydrophobic side chains in the InhA pocket. **Conclusion:** The four newly identified InhA inhibitors reported in this study could serve as promising hit compounds against *Mycobacterium tuberculosis* and may be considered for further experimental studies.

Graphical abstract:

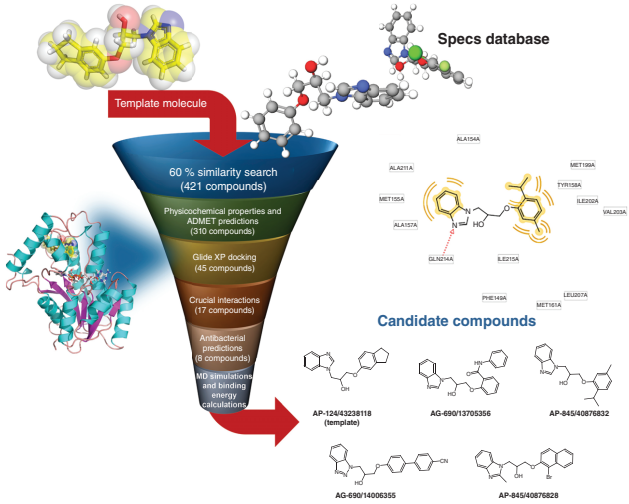

newlands press

First draft submitted: 21 December 2021; Accepted for publication: 7 March 2022; Published online: 29 April 2022

Keywords: antibacterial prediction • glide docking • InhA inhibitor • MM-GBSA • MM-PBSA • *Mycobacterium tuberculosis* • virtual screening • WaterSwap

Tuberculosis (TB) caused by *Mycobacterium tuberculosis* (*M. tuberculosis*) is one of the most widespread diseases in the world. The upturn of TB as a public health threat was mainly due to the appearance of drug-resistant TB (DR-TB). In 2021, the WHO reports suggested that around 10 million individuals were infected with, and 1.2 million people died from, TB [1]. Enoyl-ACP reductase (InhA) catalyses the nicotinamide adenine dinucleotide (NADH)-specific reduction of 2-*trans*-enoyl-ACP in the elongation cycle of mycolic acid, the major component of the mycobacterial cell wall in the fatty acid synthase type II (FAS II) pathway [2,3]. Isoniazid (INH), the first-line drug for TB treatment, acts by inhibiting the function of InhA. INH is a prodrug that requires activation by *M. tuberculosis* catalase-peroxidase (KatG) to form a covalent bond with NAD^+ in an InhA-inhibiting, INH-NAD adduct. However, the activity of INH is reduced by mutations of KatG that prevent its activation. Nevertheless, InhA remains a validated chemotherapeutic target for the development of direct InhA inhibitors that do not require activation by KatG [4]. Some novel classes of these inhibitors have been reported, such as rhodanines [5–7], thiadiazoles [8,9], triazoles [10] and 4-hydroxy-2-pyridones [11]. However, the direct InhA inhibitors exhibit good *in vitro* inhibition against the InhA enzyme but lack activity against *M. tuberculosis* growth [12]. In the present work, ligand-based and structure-based virtual screening has been applied to select candidate InhA inhibitors from the Specs database, using the similarity search method with a previously reported active compound as a template. The physicochemical and pharmacokinetic properties of selected candidates were employed, and molecular docking calculations were applied, to filter hit compounds. Furthermore, the binding interactions of candidate inhibitors in the InhA binding pocket were analyzed and compounds showing the same binding interaction as the template molecule were selected. Antibacterial models were applied to predict the anti-mycobacterial activity of hit compounds and their pharmacokinetic properties were predicted. Molecular dynamics (MD) simulations followed by binding energy calculations were applied to understand the interactions, binding modes and binding energy of these novel candidate inhibitors in the InhA binding site. The integrated findings could provide a protocol that improves the effectiveness of screening for novel InhA inhibitors by *in silico* means.

Materials & methods

The identification of novel InhA inhibitors was conducted using ligand-based virtual screening by the similarity search method against the Specs database. Adherence to Lipinski's rule of five (RO5) [13], druglikeness properties and absorption, distribution, metabolism, excretion and toxicity (ADMET) predictions were calculated using the SwissADME [14], PreADMET [15,16] and PkCSM [17] programs and used as filters to screen new compounds. Then, structure-based virtual screening against the substrate binding site of InhA using Glide XP [18] was applied to filter the hit compounds via their docking scores and their interactions with InhA compared with those of the template molecule. Next, antibacterial activity models, including PASS prediction [19,20], AntiBac-Pred [21] and MycoCSM prediction [22], were used to identify safe and potent candidates with favorable activity against mycobacteria and acceptable values for, % caseum fractions unbound (% caseum FU) and maximum recommended tolerated dose (MRTD), respectively. Hit compounds were evaluated against the PubChem database [23] to confirm the novelty of both their structures and the biological testing results. The binding of candidate compounds to InhA was further investigated using MD simulations of their complexes, starting from the dock coordinates, using AMBER20 [24], and their binding energies were calculated using the molecular mechanics Poisson–Boltzmann surface area (MM-PBSA), molecular mechanics generalized Born surface area (MM-GBSA) [25] and WaterSwap methods [26,27].

Ligand-based virtual screening

First, (2~{*S*})-1-(benzimidazol-1-yl)-3-(2,3-dihydro-1~{*H*}-inden-5-yloxy)propan-2-ol (**AP-124/43238118**) was selected [28] as the template molecule, which was subsequently used for similarity search from Specs database. The similarity search with the cut-off value of 60% was used for screening novel InhA inhibitors. The free software SwissADME [14] was used to explore physicochemical parameters. Hit compounds which passed RO5 were then cut off by Ghose value [29]. This evaluation for WlogP with the range from -0.4 to 5.6 and for MW with the range from 160 g/mol to 480 g/mol were considered. Moreover, molar refractivity (MR) was identified with the range from 40 to 130, and numbers of atoms with the range from 20 to 70. According to the cutoff values by Veber [30] for

topological polar surface area (TPSA), the values should be ≤140 Å^2 and ≤10 Å^2, respectively. Compounds that met all criteria were further investigated by docking calculations and simulations to estimate the binding affinity in the InhA binding site.

Structure-based virtual screening

The screened compounds were docked into InhA using the Glide program in the extra precision (XP) mode [18] to search for novel InhA inhibitors. The X-ray structure of InhA in complex with the relevant template compound was extracted from the Protein Data Bank (PDB code: 6R9W) [28]. The protein preparation wizard workflow was employed to prepare the receptor with PROPKA at pH 6.8 for amino acid protonation assignment. The structure was optimized using the OPLS-2005 force field [31,32] by minimization with heavy atoms restrained, giving a root-mean-square deviation (RMSD) of 0.3 Å. Finally, the optimized coordinates of InhA were placed in a box of 20 × 20 × 20 Å^3. Grid box was set by the default protocol and centered by the ligand. After sorting the compounds as described above (ligand-based virtual screening), hit compounds were used in ligand preparation for docking calculations with the Ligprep module. All conformations were minimized and a maximum of 32 conformations per ligand produced using the OPLS-2005 force field. The missing hydrogen atoms were added, and the protonation states of candidate compounds were generated with Epik at pH of 7.0 ± 2.0. For docking calculations, the InhA structure was fixed, while the compounds were freely relaxed. The threshold distance of 1 Å for clustering these binding modes was set for molecular docking calculations. Complexes with a docking score better than that of the template compound were selected as hits. Then, hit compounds were analyzed to identify their binding mode and binding interaction.

ADMET & toxicity predictions

The pharmacokinetic or ADMET properties of small molecules were calculated using SwissADME [14], PreADMET [15,16] and PkCSM [17] software and used to select novel InhA inhibitors.

Antibacterial predictions

All selected compounds predicted to be active as potential anti-TB agents using the antibacterial prediction software were collected as hit compounds for future investigations. The descriptions of active compounds for each prediction tool are provided below. In addition, biological activity against *M. tuberculosis* and InhA, as reported in the PubChem database, was investigated to ensure that the collected compounds from this virtual screening are novel and possess good biological activity. The first prediction is the PASS prediction of anti-mycobacterial activity, where compounds showing values of probability of being active (P_a) greater than the probability of being inactive (P_i) are regarded as possibly active candidates [19,20]. The second method, AntiBac-Pred, was applied to predict the anti-mycobacterial and anti-non-tuberculous mycobacteria (NTM) activity with confidence values [21]. The compounds that showed higher confidence values than those of the template compound were selected as candidates for future analysis. The third method was MycoCSM prediction [22]. In this study, the value of anti-mycobacterial activity, anti-NTM activity, % caseum FU and MRTD for candidate compounds were elucidated.

MD simulations

MD simulations were performed with the AMBER20 package [24] to predict the binding energy, binding modes and binding interactions of hit compounds in the InhA binding pocket. The *ff03* force field was used for InhA [33]. The general Amber force field (GAFF) [34] was used to generate parameters for hit compounds; those for NAD^+ cofactor were generated by the Antechamber module. Restrained electrostatic potential (RESP) [35] partial charges were calculated at HF/6-31G* for atomic charges of NAD^+ cofactor and hit compounds using Gaussian09 [36]. The TIP3P water model [37] and five Na^+ ions were chosen to represent water, for solvating, and ions, for neutralizing the system, respectively. Nine complexes, including those of the template and hit compounds in the InhA binding pocket, were first minimized by 5000 steps with the restraint force constant of 500 kcal/mol Å^2 using the steepest descent method, followed by the conjugate gradient method. The threshold value of the energy gradient for convergence was set as 0.001 kcal/mol Å^2. Then, the systems were gradually warmed from 0 to 300 K in the first 30 ps, followed by maintaining the temperature at 300 K for the last 10 ps with 2 fs simulation steps in a constant volume boundary. The selected candidates complexed with InhA were restrained to their initial coordinate structures with a weak force constant of 10 kcal/mol Å^2 during these changes in temperature. This was followed by 270 ps of position-restrained dynamics simulation with a restraint weight of 2 kcal/mol Å^2 at 300 K under an isobaric

condition. Finally, 100 ns MD simulations without any restraints were performed using the same conditions. Long-range electrostatic interactions were applied using the particle mesh Ewald (PME) method [38]. The cut-off distance for van der Waals interaction was set to 8 Å. The SHAKE method [39] was applied to constrain the bond lengths of hydrogen atoms attached to heteroatoms. The RMSDs of InhA, NAD^+ and candidate compounds were calculated over the simulation times to show the stability of the system. To evaluate the binding affinity of hit compounds bound to the InhA binding site, binding energies were employed. A representative binding mode of InhA/NAD^+/ligand complexes was obtained from clustering analysis combined with H-bond analysis to investigate the crucial interactions among the ligand, NAD^+ cofactor and amino acid in the InhA binding site.

Binding energy calculations

MM-PBSA & MM-GBSA calculations

MM-PBSA and MM-GBSA methods [25] were employed to calculate the binding energies (ΔG_{bind}) of eight hit compounds and the template molecule complexed with InhA. The atomic radii developed by Onufriev and co-workers (igb = 5) were chosen for all GB calculations [40]. The various energy terms of complexes, receptors and ligands derived from snapshots were calculated by the MM-PBSA and MM-GBSA methods. In this calculation, 1750 snapshots after equilibration had been reached (last 70 ns) were used as the coordinates for MM-PBSA and MM-GBSA calculations to get more reliable predictions of binding affinity in the InhA binding site. The binding energy (ΔG_{bind}) was calculated from Equation 1.

$$\Delta G_{bind} = \Delta G_{com} - (\Delta G_{rec} + \Delta G_{lig}) \quad \text{(Equation 1)}$$

where ΔG_{com}, ΔG_{rec} and ΔG_{lig} are the free energies of complexes, receptors and ligands for InhA complexed with hit compounds, respectively.

WaterSwap calculations

WaterSwap calculations were performed to estimate the binding energies of eight candidate compounds in the InhA binding pocket using the Sire program [26,27]. The structures of complexes obtained from the final snapshot of position-restrained MD simulations were used as the starting structure for WaterSwap calculations. Default parameters were set up to calculate the binding energy. A total of 1000 iterations were performed using sampling size for Monte Carlo simulation set to 1.6×10^9 with a replica exchange thermodynamic integration. Four highly efficient binding free energy methods, including Bennett's ratio, free energy perturbation (FEP), thermodynamic integration (TI) and quadrature-based integration of TI, were used. Agreement of <1 kcal/mol among these is regarded as reasonable and indicates the highly stable nature of the complex.

Results & discussion

Virtual screening workflow

The virtual screening protocol is summarized in Figure 1. The similarity search on the freely available commercial Specs database with the cut-off value of 60% compared with the template compound (the x-ray ligand) from the literature was applied for screening novel InhA inhibitors, and 421 compounds were obtained. Then, all compounds were filtered by RO5, Ghose and Veber using SwissADME software. In addition, ADMET parameters were applied to filter compounds using PreADMET and PkCSM free software. Consequently, 310 compounds were obtained. Molecular docking calculations of these candidate compounds were performed using Glide XP to provide the docking scores, binding modes and binding interactions of the candidate compounds in the InhA binding pocket. The docking score of the template molecule was -10.3 kcal/mol, but few candidate compounds possessed docking scores lower than that of the template molecule. Therefore, to obtain the diversity and novelty of the structures, the docking score was selected at -9.0 kcal/mol as a criterion to filter the candidate compounds. 45 candidate compounds with docking scores ranging from -9.1 to -10.7 kcal/mol were selected. The binding modes and crucial interactions in the InhA active site, including H-bond (a water-mediated H-bond to the backbone carbonyl of Ala211) and hydrophobic interactions, of these 45 candidate compounds were analyzed. Accordingly, 17 compounds with high docking scores and the same crucial interactions as the template molecule were selected. Anti-TB activity predictions were performed using PASS prediction, AntiBac-Pred and MycoCSM prediction. In addition, the PubChem database was used to check the anti-TB activity and to confirm the novelty of the candidate compounds in terms of their structures and biological activities. The results indicated that eight compounds would be expected to show biological activity against *M. tuberculosis*. MD simulations and binding energy calculations

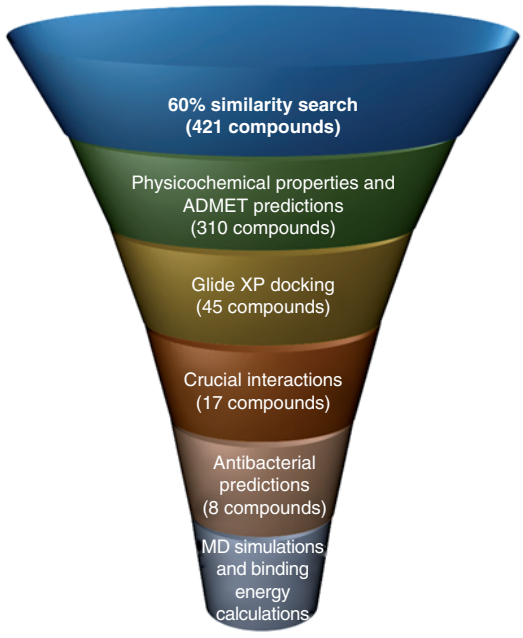

Figure 1. Virtual screening workflow used here to identify molecules as potential InhA inhibitors.
ADMET: Adsorption, distribution, metabolism, excretion and toxicity; MD: Molecular dynamics.

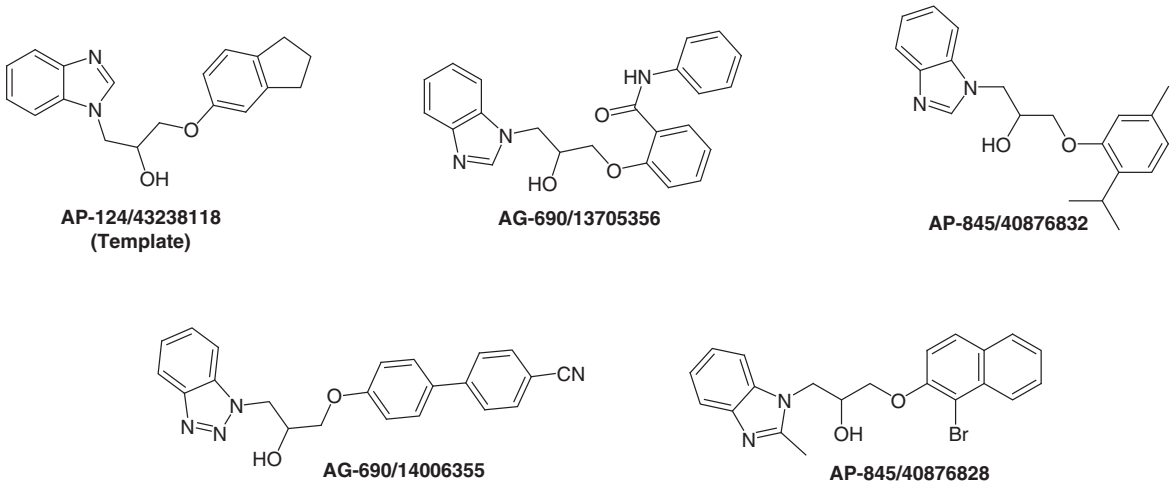

Figure 2. Structures of four potential candidates.

were performed, and the results, based on compound binding, showed that four candidate compounds met the criteria and were collected as novel candidate InhA inhibitors and anti-TB agents. The structures of these candidate compounds are summarized in Figure 2.

Physicochemical property prediction

The physicochemical properties of the eight hit compounds with predicted biological activity are summarized in Table 1. All hit compounds agreed well with RO5, with their MWs in the range from 282 to 411 g/mol. The partition coefficients (logP) were in the range from 1.8 to 3.2. The maximum numbers of hydrogen bond donors (HBD) and hydrogen bond acceptors (HBA) were 1 and 5, respectively. In addition, Ghose filter and Veber rule were also elucidated. One important parameter for the oral bioavailability is MR described by the Ghose filter. In this study, the MR values of candidate compounds showed moderate oral bioavailability, which were in the range from 82.2 to 112.0. The predicted TPSA for eight candidate compounds ranged from 47.3 to 84.0 $Å^2$. According to the cut-off values set for TPSA ($\leq$140 $Å^2$) by Veber, in comparison with the template molecule (TPSA = 47.3 $Å^2$), the candidate compounds showed TPSA values higher than that of the template molecule. These predicted TPSA values appear acceptable. The candidate compounds in this study are thus likely to have

Table 1. Summary of physicochemical properties of hit compounds.

ID number	Docking score (kcal/mol)	Physicochemical properties						
		MW (g/mol)	Rotatable bonds	Hydrogen bond acceptors	Hydrogen bond donors	logP	Topological polar surface area (Å^2)	Molar refractivity
AP-124/43238118 (template)	-10.3	308	5	3	1	2.6	47.3	90.4
AE-848/34504008	-9.4	282	6	3	1	1.8	47.3	82.2
AG-690/13705356	-10.7	354	8	5	0	2.2	76.4	112.0
AG-690/14006355	-10.8	370	6	5	1	2.5	84.0	105.7
AP-845/40876825	-9.8	314	5	4	1	2.7	47.3	87.7
AP-845/40876827	-10.3	397	5	3	1	3.2	47.3	103.0
AP-845/40876828	-9.9	411	5	3	1	3.4	47.3	108.0
AP-845/40876832	-10.6	324	6	3	1	2.8	47.3	97.3
AS-871/41615872	-9.2	338	7	4	1	1.9	64.4	97.8

MW: Molecular weight.

Table 2. Summary of absorption, distribution, metabolism, excretion and toxicity predictions of hit compounds.

ADMET parameters	AP-124/43238118 (template)	AE-848/34504008	AG-690/13705356	AG-690/14006355	AP-845/40876825	AP-845/40876827	AP-845/40876828	AP-845/40876832	AS-871/41615872
BBB	0.8	0.3	0.2	0.5	0.9	0.7	0.9	1.6	0.1
Caco-2 cell	41.1	35.6	49.4	12.3	56.5	45.4	46.5	42.4	38.1
MDCK cell	90.8	169.9	0.1	4.7	4.0	0.1	0.1	3.8	27.8
HIA	96.3	96.2	95.8	96.6	96.2	97.1	97.1	96.4	96.3
CYP3A4	Inhibitor	Inhibitor	None	Inhibitor	Inhibitor	Inhibitor	Inhibitor	Inhibitor	Inhibitor
CYP2D6	None	None	None	None	None	None	None	None	None
CYP2C9	Inhibitor	Inhibitor	Inhibitor	Inhibitor	Inhibitor	Inhibitor	Inhibitor	Inhibitor	Inhibitor
CYP2C19	Inhibitor	Inhibitor	Non	Inhibitor	Inhibitor	Inhibitor	Inhibitor	Inhibitor	Inhibitor
Ames test	Mutagen	Mutagen	Mutagen	Mutagen	Mutagen	Mutagen	Mutagen	Mutagen	Mutagen
Carcino-mouse	Negative	Negative	Negative	Negative	Negative	Negative	Negative	Negative	Negative
Carcino-rat	Negative	Positive	Negative	Negative	Positive	Positive	Positive	Negative	Negative
Hepatotoxicity	Yes	Yes	Yes	Yes	Yes	Yes	Yes	Yes	Yes

ADMET: Absorption, distribution, metabolism, excretion and toxicity; BBB: Blood–brain barrier; HIA: Human intestinal absorption; MDCK: Madin–Darby canine kidney.

a high probability of oral bioavailability. Overall, the eight hit compounds can be considered to fall within a reasonable range of physicochemical properties.

ADMET prediction

In the present study, pharmacokinetic properties (ADMET) were predicted using the PreADMET tool. In addition, the hepatotoxicity of the candidate compounds was obtained from PkCSM calculations. All ADMET parameters of these eight hit compounds are summarized in Table 2. For Caco-2 cells, five hit compounds showed higher values than that of the template molecule. This demonstrates that these compounds are expected to moderate permeability. All candidate compounds showed a lower number of Madin–Darby canine kidney (MDCK) cells than that of the template molecule, except for compound AE-848/34504008. This indicates that the candidate compounds should have good oral drug absorption and skin permeability. In addition, all eight candidate compounds showed Human intestinal absorption (HIA) values close to that of the template molecule. Higher HIA values indicate that the compounds are better absorbed from the intestinal tract upon oral administration. For distribution, the blood–brain barrier (BBB) prediction illustrated that five hit compounds, including AG-690/14006355, AP-845/40876825, AP-845/40876827, AP-845/40876828 and AP-845/40876832, showed BBB values higher than that of the template molecule. This indicates that these compounds possess moderate adsorption properties, while AE-848/34504008, AG-690/13705356 and AS-871/41615872 have lower adsorption properties. For

Table 3. Antibacterial activities of hit compounds.

Compounds	Antibacterial activities						
	PASS prediction		AntiBac-Pred		MycoCSM		
	Anti-mycobacterial		Antibacterial	Confidence	*M. tuberculosis*	Caseum FU (%)	Maximum recommended tolerated doseLog (mg/kg/day)
	P_a	P_i					
AP-124/43238118 (template)	0.2	0.2	*M. tuberculosis* H37Rv	0.1	-4.9	4.1	0.6
AE-848/34504008	0.4	0.1	*M. tuberculosis* H37Rv	0.2	-5.1	5.1	0.9
AG-690/13705356	0.3	0.1	*M. tuberculosis* H37Rv	0.1	-5.4	1.8	0.4
AG-690/14006355	None	None	None	None	-4.4	0.4	0.3
AP-845/40876825	0.3	0.1	*M. tuberculosis* H37Rv	0.1	-4.9	4.9	0.9
AP-845/40876827	None	None	None	None	-4.9	0.6	0.6
AP-845/40876828	None	None	None	None	-4.7	0.4	0.5
AP-845/40876832	0.3	0.1	None	None	-4.8	1.0	0.8
AS-871/41615872	0.3	0.1	*M. bovis*	0.1	-4.9	2.6	0.3

metabolism properties, activity toward cytochrome P450s, including CYP3A4, CYP2D6, CYP2C9 and CYP2C19, was predicted. The results indicated that most candidate compounds passed the CYP3A4 and CYP2C19 inhibition screening, except for compound ID AG-690/13705356, which is inactive toward these families. For CYP2D6, all candidate compounds showed non-inhibitory activity. For the Ames test, all candidate compounds exhibited mutagenicity, which means that all candidate compounds are mutagenic. When focusing on Carcino-rat and Carcino-mouse, all compounds were predicted to be negative, except compounds AP-845/40876825, AP-845/40876827 and AP-845/40876828, which that showed the positive prediction for the Carcino-mouse model. In addition, hepatotoxicity prediction indicated that all hit compounds and the template molecule have the predicted liver toxicity effects.

Antibacterial predictions

The predicted biological activities of hit compounds based on anti-TB and anti-NTM predictions are summarized in Table 3, Table S1 & Table S2. The anti-mycobacterium activity results of the PASS prediction suggested that five hit compounds, excepting compounds AG-690/14006355, AP-845/40876827 and AP-845/40876828, were classified as active compounds (Table 3). Based on AntiBac-Pred, the results revealed that three hit compounds showed *M. tuberculosis* H37Rv activity with higher confidence values than that of the template molecule. Moreover, compounds AS-871/41615872 (*Mycobacterium bovis*) and AP-845/40876832 (*Mycobacterium avium complex*) were predicted to have anti-NTM activity (Table 3 & Table S1). MycoCSM software was also used to identify compounds likely to be active against *M. tuberculosis* and NTM (Table 3 & Table S2). Five hit compounds were predicted to have higher activity against *M. tuberculosis* than the template molecule, the exceptions being AP-845/40876827, AP-845/40876828 and AG-690/14006355. In addition, six compounds, AS-871/41615872, AP-845/40876827, AP-845/40876828, AP-845/40876832, AG-690/13705356 and AG-690/14006355**,** showed higher anti-NTM activity than the template molecule against *Mycobacterium smegmatis*. For % caseum FU, low value showed good fraction unbound and more potent anti-TB agents. The % caseum FU predictions (Table 2) suggested that all eight compounds were more potent anti-TB agents than the template compound. Based on these results, the MRTD values of three candidate compounds, including AG-690/13705356, AG-690/14006355 and AS-871/41615872, passed the acceptable criteria while being lower than that of the template molecule. Therefore, the integrated results could provide specific information to get more specific InhA inhibitors with high potential as anti-TB agents.

The binding energies of novel InhA inhibitors

The calculated RMSD value for each solute species (InhA, NAD^+ and ligand) during MD simulations, compared with the initial docked coordinates, was calculated and plotted as shown in Figure S1. MD simulations of all systems reached the equilibrium state after 30 ns of MD simulations. The average RMSD values during the last 70 ns of the simulations ranged from 2.7 ± 0.1 Å to 3.1 ± 0.4 Å for InhA, 1.5 ± 0.2 Å to 2.0 ± 0.3 Å for NAD^+

Table 4. The binding energies of InhA inhibitors calculated by molecular mechanics Poisson–Boltzmann surface area, molecular mechanics Generalized Born surface area and WaterSwap methods.

Compounds	ΔG_{bind} (kcal/mol)		
	MM-PBSA	MM-GBSA	WaterSwap
AP-124/43238118 (template)	-11.8 ± 3.0	-33.6 ± 3.4	-25.7 ± 0.5
AE-848/34504008	-17.3 ± 4.0	-32.1 ± 3.9	-21.0 ± 0.7
AG-690/13705356	-21.4 ± 2.9	-37.1 ± 3.8	-27.0 ± 0.4
AS-871/41615872	-15.8 ± 3.5	-32.8 ± 3.9	-19.3 ± 0.2
AG-690/14006355	-18.6 ± 5.3	-35.4 ± 6.9	-30.1 ± 0.8
AP-845/40876825	-11.6 ± 3.1	-30.9 ± 4.4	-21.8 ± 1.1
AP-845/40876827	-14.6 ± 4.3	-27.0 ± 6.5	-30.2 ± 0.7
AP-845/40876828	-12.3 ± 3.3	-33.6 ± 6.6	-28.5 ± 0.2
AP-845/40876832	-20.1 ± 3.3	-35.7 ± 3.8	-26.3 ± 0.6

MM-GBSA: Molecular mechanics Generalized Born surface area; MM-PBSA: Molecular mechanics Poisson–Boltzmann surface area.

and 2.4 ± 0.6 Å to 3.0 ± 0.3 Å for ligands. Eight hit compounds and the template molecule were investigated for their binding energies in the InhA binding pocket by MM-PBSA, MM-GBSA and WaterSwap methods as shown in Table 4. The lowest binding energies were those of **AG-690/13705356** (-21.4 ± 2.9 kcal/mol for MM-PBSA and -37.1 ± 3.8 kcal/mol for MM-GBSA) and **AP-845/40876827** (-30.2 ± 0.7 kcal/mol for WaterSwap), respectively. Thus, these candidate compounds showed binding energies lower than that of the template. Therefore, four compounds, **AG-690/13705356**, **AG-690/14006355**, **AP-845/40876828** and **AP-845/40876832**, with binding energies lower than that of the template compound were selected to investigate the binding mode and binding interactions.

Binding mode & binding interaction of candidate compounds

Various factors, including physicochemical and pharmacokinetic properties, docking scores, and binding energies, compared with those of the template molecule were considered and four candidate compounds, including compounds **AG-690/13705356**, **AG-690/14006355**, **AP-845/40876828** and **AP-845/40876832**, were further utilized for investigation of their InhA interactions and binding affinity. Schematic representations of the candidate compounds in the InhA binding site, as derived from MD simulations, are shown in Figures 3 & 4. Based on pharmacophore analysis by means of automated structure-based model generation using LigandScout [42] of the template molecule and candidate compounds, it was found that H-bond interactions and hydrophobic interactions were crucial for binding in the InhA binding site (Figure 4). The hydroxy group (OH) of the propan-2-ol moiety played an important role in the H-bond interaction with water, NAD^+ and amino acids in the InhA binding site. H-bond interactions of the template and candidate compounds derived from MD simulations are summarized in Table S3. For example, the OH of the template molecule, whose binding to InhA was established by X-ray crystallography as described in our previous report, showed a water-mediated H-bond to the backbone carbonyl of Ala211 (Figure 4A) [28]. On the other hand, the H-bond between the template and Ala211 via a water-mediated interaction was lost after MD simulation. The OH of the template interacted with an oxygen atom of the pyrophosphate group of NAD^+, as shown in Figures 3A & 4B. This H-bond was occupied for more than 80% of the simulation. The average distances were 2.60 Å and 2.68 Å from the OH of ligand to O1N (79.5% occupancy) and O2A (13.8% occupancy) on the pyrophosphate group of NAD^+, respectively. In addition, the equivalent OH group of compounds **AG-690/14006355** and **AP-845/40876828** formed H-bond interactions with Gln214 (24.0% occupancy, 2.70 Å) (Figures 3C & 4D) and the NAD^+ cofactor (44.4% occupancy, 2.63 Å) (Figures 3E & 4F), respectively. The average distances from the OH of **AG-690/14006355** and **AP-845/40876828** to the NH side chain of Gln214 were 2.89 Å and 2.63 Å, respectively. These findings suggested that the OH on the propan-2-ol moiety of the candidate compounds was important for binding in the InhA binding site. Only two compounds, **AG-690/13705356** and **AP-845/40876832**, showed different H-bond interactions with amino acids in the InhA binding site. A carbonyl oxygen of **AG-690/13705356** contacted the NH side chain of Gln214 with an average distance value of 2.89 Å (24.2% occupancy), and the nitrogen atom in the benzimidazole ring of **AP-845/40876832** formed H-bond interactions with the side chain of Gln214 with an average distance value of 2.92 Å (5.4% occupancy). Due to the hydrophobic properties of the InhA binding site (66% hydrophobic

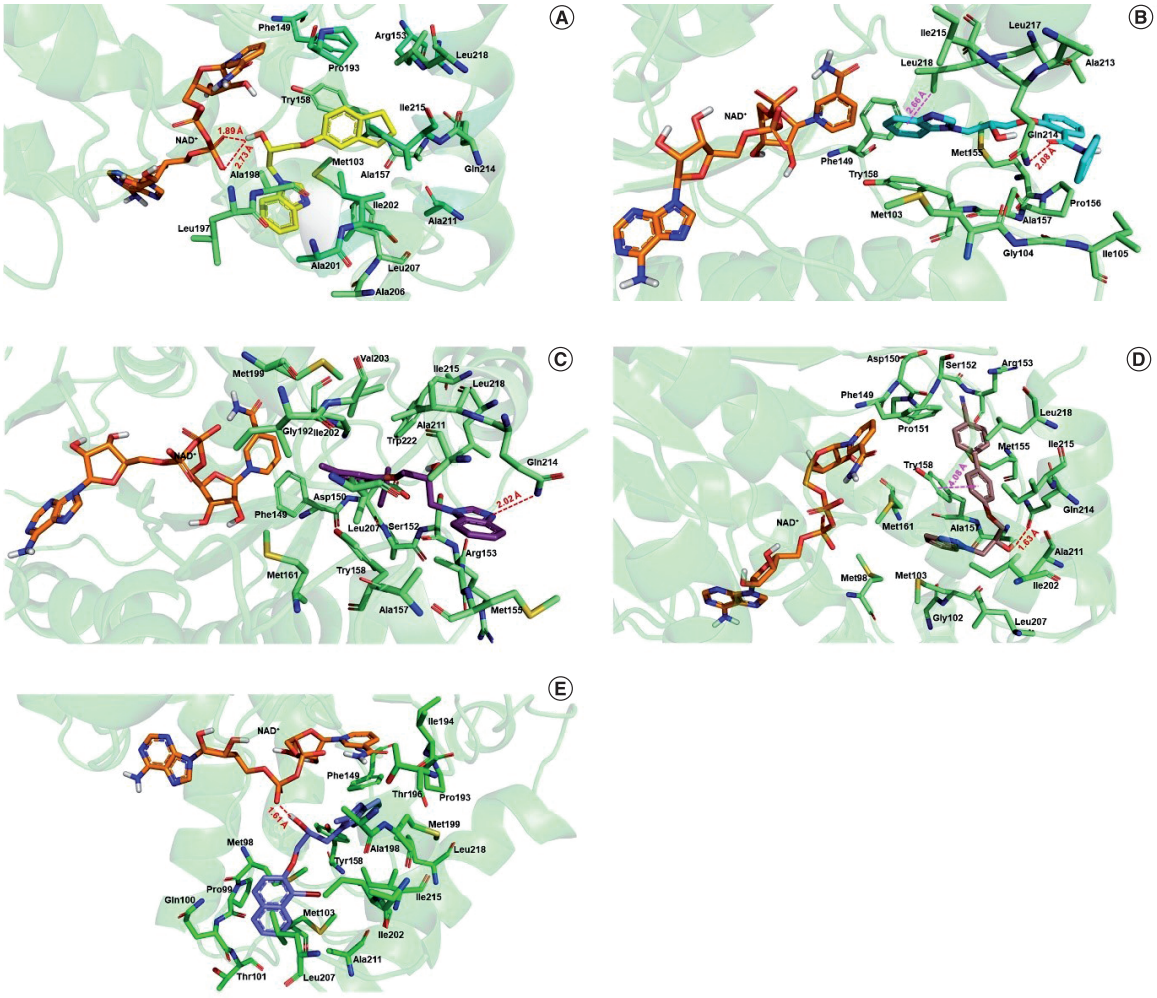

Figure 3. (A) Binding mode of the template molecule. **(B)** AG-690/13705356. **(C)** AP-845/40876832. **(D)** AG-690/14006355. **(E)** AP-845/40876828 complexed with InhA. InhA–ligand complexes were modeled by molecular dynamics simulations. Red and pink dashed lines indicate H-bond and pi–pi interactions, respectively.

residues in the substrate binding site) [41], the results from both x-ray crystallography and MD simulations showed that the bicyclic indane of the template is bound in an extended hydrophobic pocket contacting residues Phe149, Met155, Ala157, Tyr158, Ile215 and Leu218, while the benzimidazole ring contacts residues Met103, Ala198, Ala201 and Ile202 (Figure 3A & B). The same hydrophobic features were observed for all candidate compounds in the InhA binding site, as displayed in yellow on the benzimidazole ring and phenyl scaffold in the modeled complexes after MD simulations. Based on the hydrophobic features of the benzimidazole and phenyl rings of the candidate compounds from 2D pharmacophore analysis, additional interactions potentially crucial for the binding of the candidate compounds were analyzed. Both pi–pi and sigma–pi interactions contribute to the binding affinity of the candidate compounds. The benzimidazole ring of **AG-690/13705356** formed a sigma–pi interaction with the Leu218 side chain (2.83 Å) (Figure 3B). The phenyl ring on the 4′-cyano-biphenyl of **AG-690/14006355** contacted the Tyr158 side chain via pi–pi interactions (4.08 Å) (Figure 3D). As mentioned earlier, all candidate compounds were found to form strong interactions in the InhA binding pocket and to show promising properties with respect to interaction with InhA and suitability to act as anti-TB agents based on the physicochemical properties, antibacterial activities and pharmacokinetic predictions.

Conclusion

In conclusion, new potential InhA inhibitors were identified by ligand-based and structure-based virtual screening of a commercial database. The validated models were exploited for virtual screening and the candidate compounds were

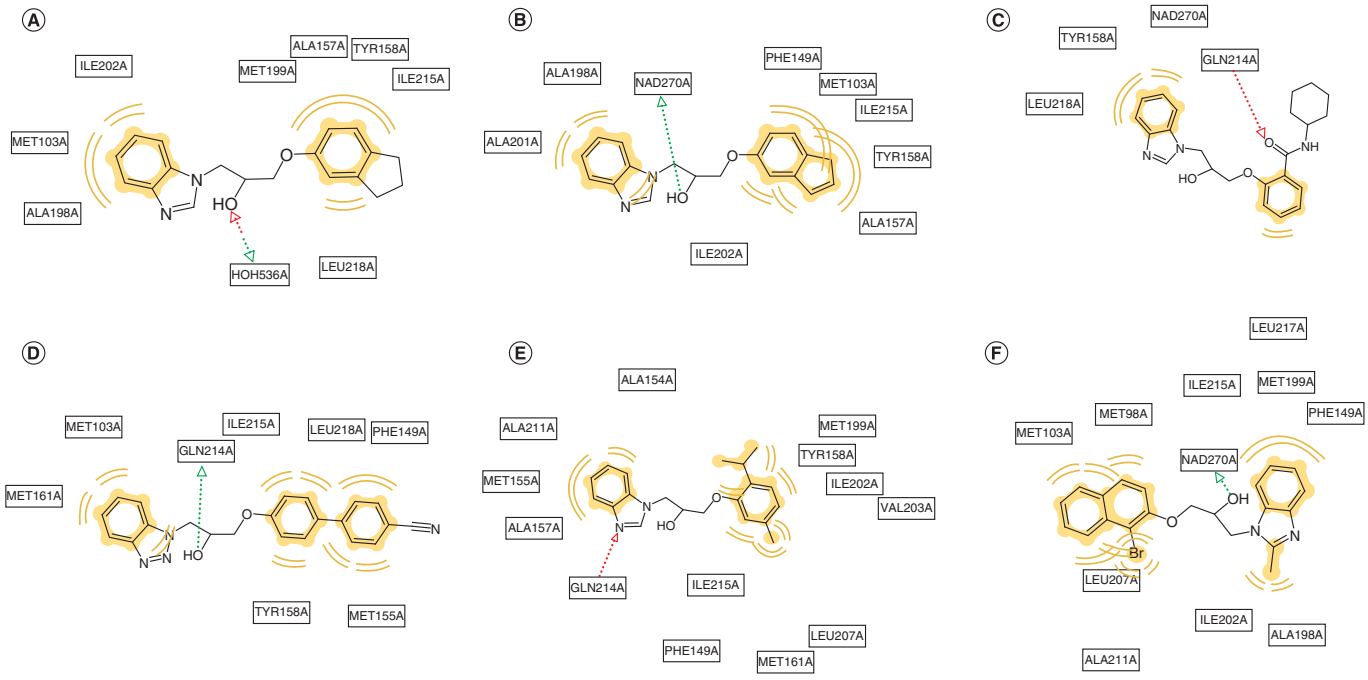

Figure 4. The 2D pharmacophore features of candidate compounds generated from LigandScout. (A) Template x-ray conformation. **(B)** Molecular dynamics simulation conformation. **(C)** AG-690/13705356. **(D)** AP-845/40876832. **(E)** AG-690/14006355 **(F)** AP-845/40876828.

filtered and scored by employing pharmacokinetic and physicochemical property filters and docking studies. Their antibacterial activities were also predicted. In addition, binding energy calculations using MM-PBSA, MM-GBSA and WaterSwap methods were performed for the screened compounds. Four candidate compounds, including AG-690/13705356, AG-690/14006355, AP-845/40876828 and AP-845/40876832, are predicted to bind to InhA and to have anti-mycobacterial activity. The binding affinity calculations indicated the selected compounds (AG-690/13705356, AG-690/14006355, AP-845/40876828 and AP-845/40876832) better to InhA than the template compound. The interactions of the candidate compounds with the InhA binding pocket include H-bond, pi–pi, sigma–pi and hydrophobic interactions. These data suggest that the compounds identified in this study may have anti-TB activities through the targeting of InhA and are consequently worthy of experimental study.

Future perspective

Nowadays, the development of multidrug-resistant TB and extensively drug-resistant TB is a big challenge in the control of TB infections. Therefore, the development of novel anti-TB drugs is urgently required. This study successfully applied the virtual screening approach to screening for novel InhA inhibitors. The results identify promising candidates as anti-TB compounds. These integrated computational methods are reliable tools for screening for hit compounds against InhA that warrant further experimental studies. The results could provide important guidelines and design insights for future studies for the development of novel selective direct InhA inhibitors.

Summary points

- Candidate compounds were screened from the Specs database by ligand- and structure-based virtual screening.
- Glide XP docking, molecular mechanics Generalized Born surface area, molecular mechanics Poisson–Boltzmann surface area and WaterSwap methods were used to investigate the binding mode, binding interaction and binding energy of candidate compounds in the InhA binding site.
- Four candidates are potential hit compounds, exhibiting binding energies lower than that of the template molecule (i.e., higher binding affinity) and are worthy of further experimental investigation.

Acknowledgments

The authors would like to thank the Center of Excellence for Innovation in Chemistry (PERCH-CIC), Faculty of Science, Ubon Ratchathani University, Faculty of Science, Nakhon Phanom University, Faculty of Science, Kasetsart University, and University of Bristol for their support and facilities. The National Electronics and Computer Technology Center (NECTEC) and the National Nanotechnology Center (NANOTEC) are also gratefully acknowledged for supporting this research.

Financial & competing interests disclosure

This research was supported by the Thailand Research Fund (RSA5980057), RGJ Advanced Programme (RAP60K0009), Ubon Ratchathani University and the Thailand Graduate Institute of Science and Technology (TGIST) (SCA-CO-2560-4375TH and SCA-CO-2563-12135-TH) to C Hanwarinroj and N Phusi, respectively. The financial support from Royal Golden Jubilee PhD Program to B Kamsri (PHD/0132/2559) is gratefully acknowledged. AJ Mulholland and J Spencer also would like to thank the EPSRC for funding via BristolBridge (grant number EP/M027546/1) and CCP-BioSim (grant number EP/M022609/1). The authors have no other relevant affiliations or financial involvement with any organization or entity with a financial interest in or financial conflict with the subject matter or materials discussed in the manuscript apart from those disclosed.

No writing assistance was utilized in the production of this manuscript.

References

Papers of special note have been highlighted as: • of interest

1. World Health Organization. Global tuberculosis report 2021. www.who.int/publications/digital/global-tuberculosis-report-2021 (1 February 2022).
2. Rozwarski DA, Vilchèze C, Sugantino M, Bittman R, Sacchettini JC. Crystal structure of the *Mycobacterium tuberculosis* enoyl-ACP reductase, InhA, in complex with NAD^+ and a C16 fatty acyl substrate. *J. Biol. Chem.* 274(22), 15582–15589 (1999).
3. Takayama K, Wang C, Besra GS. Pathway to synthesis and processing of mycolic acids in *Mycobacterium tuberculosis*. *Clin. Microbiol. Rev.* 18(1), 81–101 (2005).
4. Prasad MS, Bhole RP, Khedekar PB, Chikhale RV. *Mycobacterium* enoyl acyl carrier protein reductase (InhA): a key target for antitubercular drug discovery. *Bioorg Chem.* 115, 105242 (2021).
5. Shaikh MS, Kanhed AM, Chandrasekaran B *et al.* Discovery of novel N-methyl carbazole tethered rhodanine derivatives as direct inhibitors of *Mycobacterium tuberculosis* InhA. *Bioorg. Med. Chem. Lett.* 29(16), 2338–2344 (2019).
6. Xu JF, Wang TT, Yuan Q *et al.* Discovery and development of novel rhodanine derivatives targeting enoyl-acyl carrier protein reductase. *Bioorg. Med. Chem.* 27(8), 1509–1516 (2019).
7. Sun ZG, Xu YJ, Xu JF, Liu QX, Yang YS, Zhu HL. Introducing broadened antibacterial activity to rhodanine derivatives targeting enoyl-acyl carrier protein reductase. *Chem. Pharm. Bull. (Tokyo)* 67(2), 125–129 (2019).
8. Doğan H, Doğan ŞD, Gündüz MG *et al.* Discovery of hydrazone containing thiadiazoles as *Mycobacterium tuberculosis* growth and enoyl acyl carrier protein reductase (InhA) inhibitors. *Eur. J. Med. Chem.* 188, 112035 (2020).
9. Mali JK, Sutar YB, Pahelkar AR, Verma PM, Telvekar VN. Novel fatty acid-thiadiazole derivatives as potential antimycobacterial agents. *Chem. Biol. Drug. Des.* 95(1), 174–181 (2020).
10. Spagnuolo LA, Eltschkner S, Yu W *et al.* Evaluating the contribution of transition-state destabilization to changes in the residence time of triazole-based InhA inhibitors. *J. Am. Chem. Soc.* 139(9), 3417–3429 (2017).
11. Manjunatha UH, Rao SPS, Kondreddi RR *et al.* Direct inhibitors of InhA are active against *Mycobacterium tuberculosis*. *Sci. Transl. Med.* 7(269), 269ra3 (2015).
12. Holas O, Ondrejcek P, Dolezal M. *Mycobacterium tuberculosis* enoyl-acyl carrier protein reductase inhibitors as potential antituberculotics: development in the past decade. *J. Enzyme. Inhib. Med. Chem.* 30(4), 629–648 (2015).
13. Lipinski CA. Lead- and drug-like compounds: the rule-of-five revolution. *Drug Discov. Today Technol.* 1(4), 337–341 (2004).

• **Discusses physicochemical properties using computational methods.**

14. Daina A, Michielin O, Zoete V. SwissADME: a free web tool to evaluate pharmacokinetics, drug-likeness and medicinal chemistry friendliness of small molecules. *Sci. Rep.* 7, 42717 (2017).

• **Discusses absorption, distribution, metabolism, excretion and toxicity prediction using computational methods.**

15. Lee SK, Chang GS, Lee IH, Chung JE, Sung KY. The PreADME: PC-based program for batch prediction of ADME properties. *Euro. QSAR* 9, 5–10 (2004).

- **Discusses absorption, distribution, metabolism, excretion and toxicity prediction using computational methods.**

16. Lee SK, Lee IH, Kim HJ, Chang GS, Chung JE, No KT. The PreADME approach: web-based program for rapid prediction of physico-chemical, drug absorption and drug-like properties. *Euro. QSAR* 418–420 (2003).

- **Discusses absorption, distribution, metabolism, excretion and toxicity prediction using computational methods.**

17. Pires DE, Blundell TL, Ascher DB. PkCSM: predicting small-molecule pharmacokinetic and toxicity properties using graph-based signatures. *J. Med. Chem.* 58(9), 4066–4072 (2015).

18. Friesner RA, Murphy RB, Repasky MP *et al.* Extra precision Glide: docking and scoring incorporating a model of hydrophobic enclosure for protein-ligand complexes. *J. Med. Chem.* 49(21), 6177–6196 (2006).

- **Discusses antibacterial activity predictions using computational methods.**

19. Lagunin A, Stepanchikova A, Filimonov D, Poroikov V. PASS: prediction of activity spectra for biologically active substances. *Bioinformatics* 16(8), 747–748 (2000).

- **Discusses antibacterial activity predictions using computational methods.**

20. Poroikov VV, Filimonov DA, Gloriozova TA *et al.* Computer-aided prediction of biological activity spectra for organic compounds: the possibilities and limitations. *Russ. Chem. Bull.* 68, 2143–2154 (2019).

- **Discusses antibacterial activity predictions using computational methods.**

21. Pogodin PV, Lagunin AA, Rudik AV, Druzhilovskiy DS, Filimonov DA, Poroikov VV. AntiBac-Pred: a web application for predicting antibacterial activity of chemical compounds. *J. Chem. Inf. Model.* 59(11), 4513–4518 (2019).

- **Discusses antibacterial activity predictions using computational methods.**

22. Pires DEV, Ascher DB. MycoCSM: using graph-based signatures to identify safe potent hits against mycobacteria. *J. Chem. Inf. Model.* 60(7), 3450–3456 (2020).

23. Kim S, Chen J, Cheng T *et al.* PubChem in 2021: new data content and improved web interfaces. *Nucleic Acids Res.* 49(D1), D1388–D1395 (2021).

24. Case DA, Aktulga HM, Belfonet K *et al.* Amber 2020. University of California, San Francisco, CA, USA (2020).

- **Discusses binding energy calculation on implicit water model using computational methods.**

25. Tuccinardi T. What is the current value of MM/PBSA and MM/GBSA methods in drug discovery? *Expert Opin. Drug Discov.* 16(11), 1233–1237 (2021).

- **Discusses binding energy calculation on explicit water model using computational methods.**

26. Woods CJ, Malaisree M, Michel J, Long B, McIntosh-Smith S, Mulholland AJ. Rapid decomposition and visualisation of protein-ligand binding free energies by residue and by water. *Faraday Discuss.* 169, 477–499 (2014).

27. Woods CJ, Malaisree M, Hannongbua S, Mulholland AJ. A water-swap reaction coordinate for the calculation of absolute protein-ligand binding free energies. *J. Chem. Phys.* 134(5), 054114 (2011).

- **Discusses computational screening to select InhA inhibitors.**

28. Kamsri P, Hanwarinroj C, Phusi N *et al.* Discovery of new and potent InhA inhibitors as antituberculosis agents: structure-based virtual screening validated by biological assays and x-ray crystallography. *J. Chem. Inf. Model.* 60(1), 226–234 (2020).

29. Ghose AK, Viswanadhan VN, Wendoloski JJ. A knowledge-based approach in designing combinatorial or medicinal chemistry libraries for drug discovery. 1. A qualitative and quantitative characterization of known drug databases. *J. Comb. Chem.* 1(1), 55–68 (1999).

30. Veber DF, Johnson SR, Cheng HY, Smith BR, Ward KW, Kopple KD. Molecular properties that influence the oral bioavailability of drug candidates. *J. Med. Chem.* 45(12), 2615–2623 (2002).

31. Jorgensen WL, Maxwell DS, Tirado RJ. Development and testing of the OPLS all-atom force field on conformational energetics and properties of organic liquids. *J. Am. Chem. Soc.* 118(45), 11225–11236 (1996).

32. Kaminski GA, Friesner RA, Tirado RJ, Jorgensen WL. Evaluation and reparametrization of the OPLS-AA force field for proteins via comparison with accurate quantum chemical calculations on peptides. *J. Phys. Chem. B* 105(28), 6474–6487 (2001).

33. Duan Y, Wu C, Chowdhury S *et al.* A point-charge force field for molecular mechanics simulations of proteins based on condensed-phase quantum mechanical calculations. *J. Comput. Chem.* 24(16), 1999–2012 (2003).

34. Wang JM, Wolf RM, Caldwell JW, Kollman PA, Case DA. Development and testing of a general AMBER force field. *J. Comput. Chem.* 25(9), 1157–1174 (2004).

35. Bayly CI, Cieplak P, Cornell W, Kollman PA. A well-behaved electrostatic potential based method using charge restraints for deriving atomic charges: the RESP model. *J. Phys. Chem.* 97(40), 10269–10280 (1993).

36. Frisch MJ, Trucks GW, Schlegel HB *et al.* Gaussian 09. Gaussian, Inc., Wallingford, CT, USA (2016).

37. Jorgensen WL, Chandrasekhar J, Madura JD, Impey RW, Klein ML. Comparison of simple potential functions for simulating liquid water. *J. Chem. Phys.* 79, 926–935 (1983).

38. Darden T, York D, Pedersen LJ. Particle mesh Ewald-an *N*·Log(*N*) method for Ewald sums in large systems. *J. Chem. Phys.* 98, 10089–10092 (1993).

39. Ryckaert JP, Ciccotti G, Berendsen HJC. Numerical integration of the Cartesian equations of motion of a system with constraints: molecular dynamics of *n*-alkanes. *J. Comput. Phys.* 23(3), 327–341 (1977).

40. Onufriev A, Bashford D, Case DA. Exploring protein native states and large-scale conformational changes with a modifed generalized born model. *Proteins* 55(2), 383–394 (2004).

41. Pauli I, Santos RND, Rostirolla DC *et al.* Discovery of new inhibitors of *Mycobacterium tuberculosis* InhA enzyme using virtual screening and a 3D-pharmacophore-based approach. *J. Chem. Inf. Model.* 53(9), 2390–2401 (2013).

42. Wolber G, Langer T. LigandScout: 3-D pharmacophores derived from protein-bound ligands and their use as virtual screening filters. *J. Chem. Inf. Model.* 45(1), 160–169 (2005).